# A NEW METHOD FOR FOCUSING AND IMAGING X-RAYS AND GAMMA-RAYS WITH DIFFRACTION CRYSTALS

Robert K. Smither
Argonne National Laboratory
Received_____

## ABSTRACT

The new method can focus monochromatic radiation from a point source or parallel beam down to a point image. Conversely, radiation from a point source can be focused into an outgoing parallel beam. The focusing to and from a parallel beam has never been achieved before with diffraction crystals. The method makes use of bent diffraction crystals in which the intercrystalline-plane spacing is varied as a function of position in the crystal. The Bragg angle for diffraction of monochromatic radiation will now vary as a function of position in the crystal and this new degree of freedom is used to obtain focusing and imaging of the diffracted beam. This new approach to focusing and imaging is applied to the design of a large-area, high resolution x-ray telescope that is also a high resolution monochromator with the unique feature that the width of the energy increment that is diffracted can be controlled and varied during the operation of the instrument. This makes it possible to first scan the field with a wide energy increment and ther switch to a narrow energy increment for the high resolution work. The new focusing system can be used with both transmission and reflection type diffraction crystals and is applicable to photons with energies from a few keV to 500 keV. High resoltion imaging (few arc sec) is possible even at the higher photon energies.

## I. INTRODUCTION

Diffraction crystals have been used for many years to focus a point or line source to a line image (Johnson, 1931) and in some special cases to focus a point source to a point image (Berreman, et al., 1954 and Berreman, 1955). A schematic drawing of the basic geometry used in these instruments is shown in Figure 1. The source, image, and bent crystal all lie on a focal circle whose

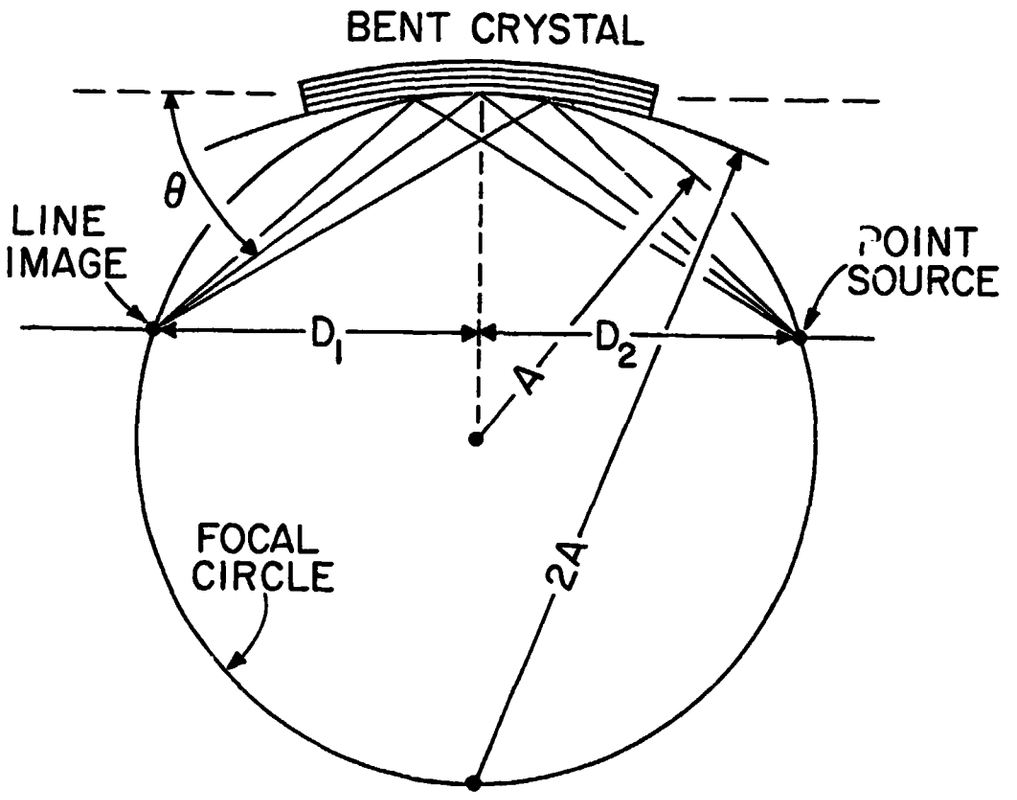


Fig. 1. Classic reflection-type focusing crystal-diffraction spectrometer. θ is the Bragg angles, "A" is the radius of the focal circle and "2A" is the radius of curvature of the bent-crystal. $D_1$ and $D_2$ are the image distance and the source distance, respectively

diameter is equal to the radius of curvature (2A) of the bent-crystal. $D_1$, the image distance in equal to $D_2$ the object distance. If the diffraction crysal is bent to a cylindrical shape the radiation will be focused to a line image. If the diffraction crystal is also bent in the direction perpendicular to the diffraction plane (the diffraction plane is the plane containing the incoming and outgoing rays) then it is possible to focus the radiation from a point source to a point image. The first type of focusing system works quite well in the laboratory when used with reasonable values for the diameter of the focal circle. A multiple crystal version of this type of instrument was used in conjunction with the grazing incidence x-ray telescope in the Einstien Observatory to do spectral analysis of the x-ray image (Canisares, et al. 1977).

This type of instrument can not be extended for use with a point source at infinite because as $D_2$, the source distance increases the value of $D_1$, the image distance increase as well and in the limit when $D_2 \to \infty$, $D_1$ also approaches infinity and the bent crystal becomes a flat crystal ($2A \to \infty$). Thus the incoming parallel beam is diffracted as a parallel outgoing beam with no focusing in the diffraction plane. The use of a transmission type diffraction spectrometer does not help (see Figure 2). Here the diffracted beam is always

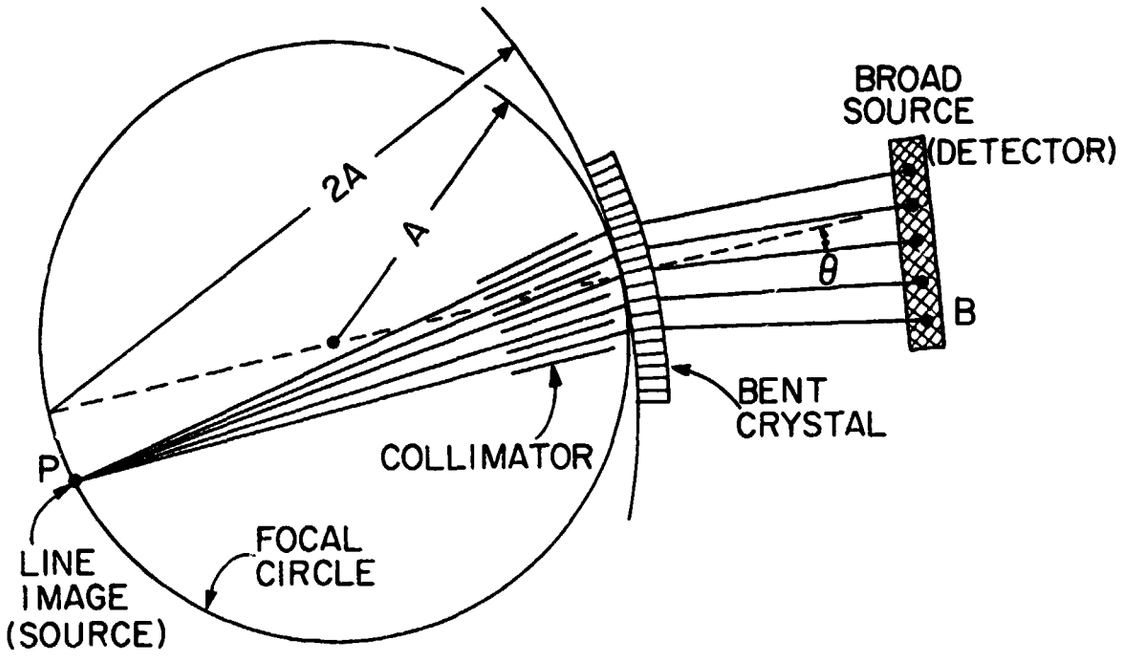


Fig. 2. Transmission-type crystal-diffraction spectrometer. "A" is the radius of the focal circle and "2A" is the radius of curveture of the bent crystal

defocused and approaches a parallel beam diffracted by a flat crystal when the source distance approaches infinity. In this mode of operation the diffraction crystal can be viewed as an excellent monochromatic collimator. Although this type of instrument is not very useful for imaging it could be used to make a spectra analysis of a large gas cloud or other extended sources. The different wavelengths would be focused at different places on the focal circle so the full spectrum could be recorded at the same time with a position sensitive detector

## II. NEW METHOD OF FOCUSING X-RAYS

The new focusing method is discussed in detail in a recent article in R.S.I. by R. K. Smither (1982). The basic approach is illustrated in Figure 3. Here a flat crystal is used to focus monochromatic radiation from a point or line source to a line image by varying the crystal "d" spacing in the diffraction crystal as a function of the distance, "x", from the baseline (line from source to image). A thermal gradient is used in this example to change the "d" spacing so that the Bragg condition:

$$n\lambda = 2d \sin \theta \tag{1}$$

is satisfied over the whole crystal surface for monochromatic radiation. If $D_1 = D_2$ this will automatically satisfy the focusing requirements as well.

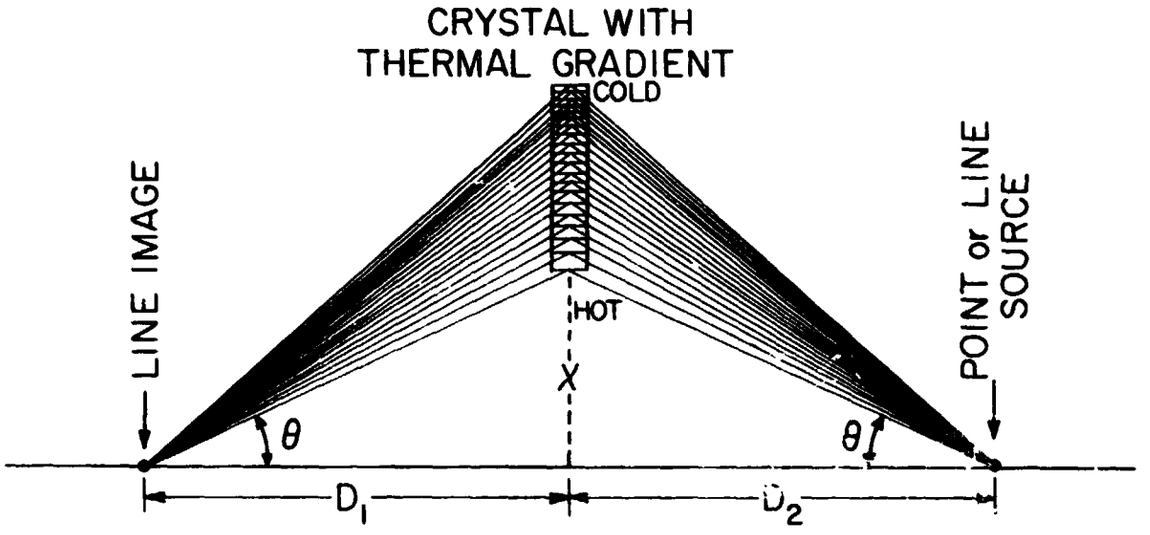


Fig. 3. New transmission type of crystal diffraction spectrometer using an unbent crystal with a thermal gradient applied to the crystal perpendicular to the diffraction planes with decreasing temperatures as x increases. The image distance, $D_1$, equals the source distance, $D_2$. $D_1$ must be equal to $D_2$ for the Bragg diffraction condition to be satisfied

The fractional change in the "d" spacing must match the fraction change in the value of sin $\theta$. Thus:

$$\Delta d/d = \Delta \sin \theta / \sin \theta = \Delta\theta \cot \theta \tag{2}$$

where $\theta$ is the Bragg angle and d the "d" spacing in the crystal. In Eq. (1), $\lambda$ is the wavelength and "n" the diffraction order.

The thermal gradient needed to achieve this diffraction focusing is given by Eq. (3)

$$\frac{\Delta t}{\Delta x} = \frac{1}{\alpha d} \cdot \frac{\Delta d}{\Delta x} = \frac{-\cos^2 \theta}{\alpha x} \tag{3}$$

where $\alpha$ is the coefficient of thermal expansion and $\Delta d/d = \alpha \Delta t$. The change in $\theta$ that can be focused is determined by the temperature differential, $\Delta t$, that is applied to the crystal. If the diffraction process uses the planes in quartz that are perpendicular to the optical axis, $\alpha$ is $1.34 \times 10^{-5}/°C$ and assuming a $\Delta t$ of 200°C this gives $\Delta d/d = 2.7 \times 10^{-3}$. If $\theta = 20°$ then $\Delta\theta = 10^{-3}$ radians or 200 arc sec. This can be compared with the two arc sec for the rocking curve or acceptance angle of a good crystal without the presence of a thermal gradient. This results in an improvement of a factor of 100 for the diffraction intensity, while at the same time obtaining good convergence of the beam. The width of the image will be equal to the width of the source and will not reflect the mosaic structure of the crystal. This last effect leads to much better imaging than one might expect and comes about because most high quality crystals are composed of many small crystallite structures whose rocking curve or diffraction resolution is much better than the width of the mosaic structure which is a measure of the relative misalignment of these crystallites.

The more general case where $D_1$ is not equal to $D_2$ is shown in Figure 4. Both the transmission case (Figure 4a) and the reflection case (Figure 4b) lead to focusing so both large and small values of 6 can be handled with ease. The transmission case acts like a cylindrical lens (the first practical lens for high energy x-rays) and the reflection case like a cylindrical mirror. Both cases require that the diffraction crystal be bent. The radius of curvature, $R_c$, which controls the rate of change in the crystal plane tilt angle, $\phi$, is given by Eq. (4) for the transmission case,

$$R_c = \frac{2R_1R_2}{(R_1-R_2)\cos\theta} \tag{4}$$

and Eq. (5) for the reflection case

$$R_c = \frac{2R_1R_2}{(R_2+R_1)\sin\theta} \tag{5}$$

where $R_1$ and $R_2$ are the distance from the image to the crystal and from the source to the crystal, respectively. $\phi$ is the angle between the crystal planes and the baseline. For a distant source $D_2$ and $R_2$ approach infinity as before but $D_1$ and $R_1$ remain finite and can be scaled up or down as one wishes so we now have two systems that will focus a parallel beam of radiation to a line image. The parallel beam focusing case is shown in Figure 5. The focal distance, $D_1$, in both cases is given by Eq. (6)

$$D_1 = x \cot 2\theta \tag{6}$$

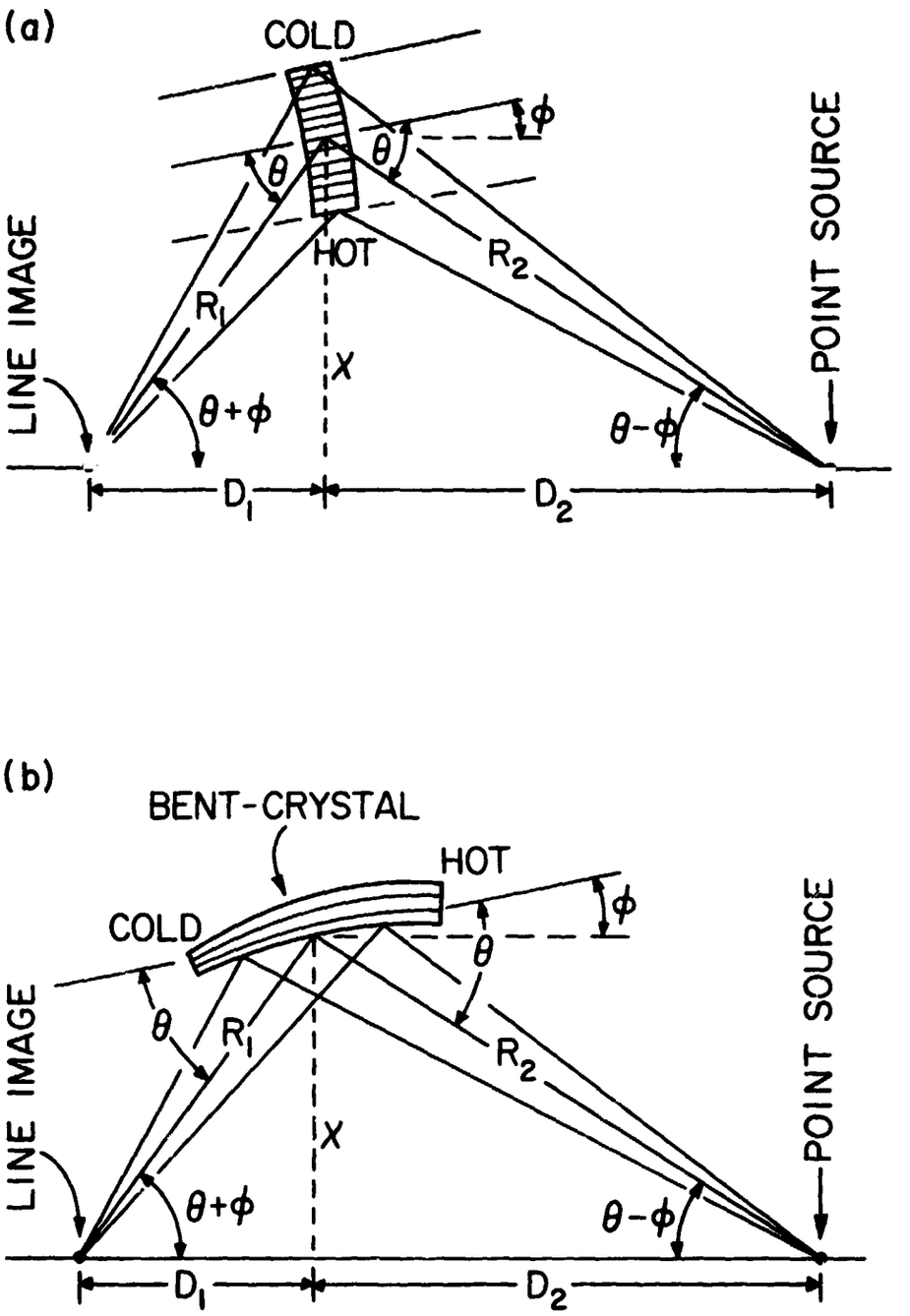


Fig. 4. (a) Transmission type and (b) reflection type diffraction spectrometer using thermal gradients and bent crystals for the general case when the image distance, $D_1$, is not equal to the source distance, $D_2$. $\phi$ is the angle of tilt of the crystal plane, x is the height of the crystal plane above the baseline, and $R_1$ and $R_2$ are the distances from the point of diffraction to the image and source, respectively.

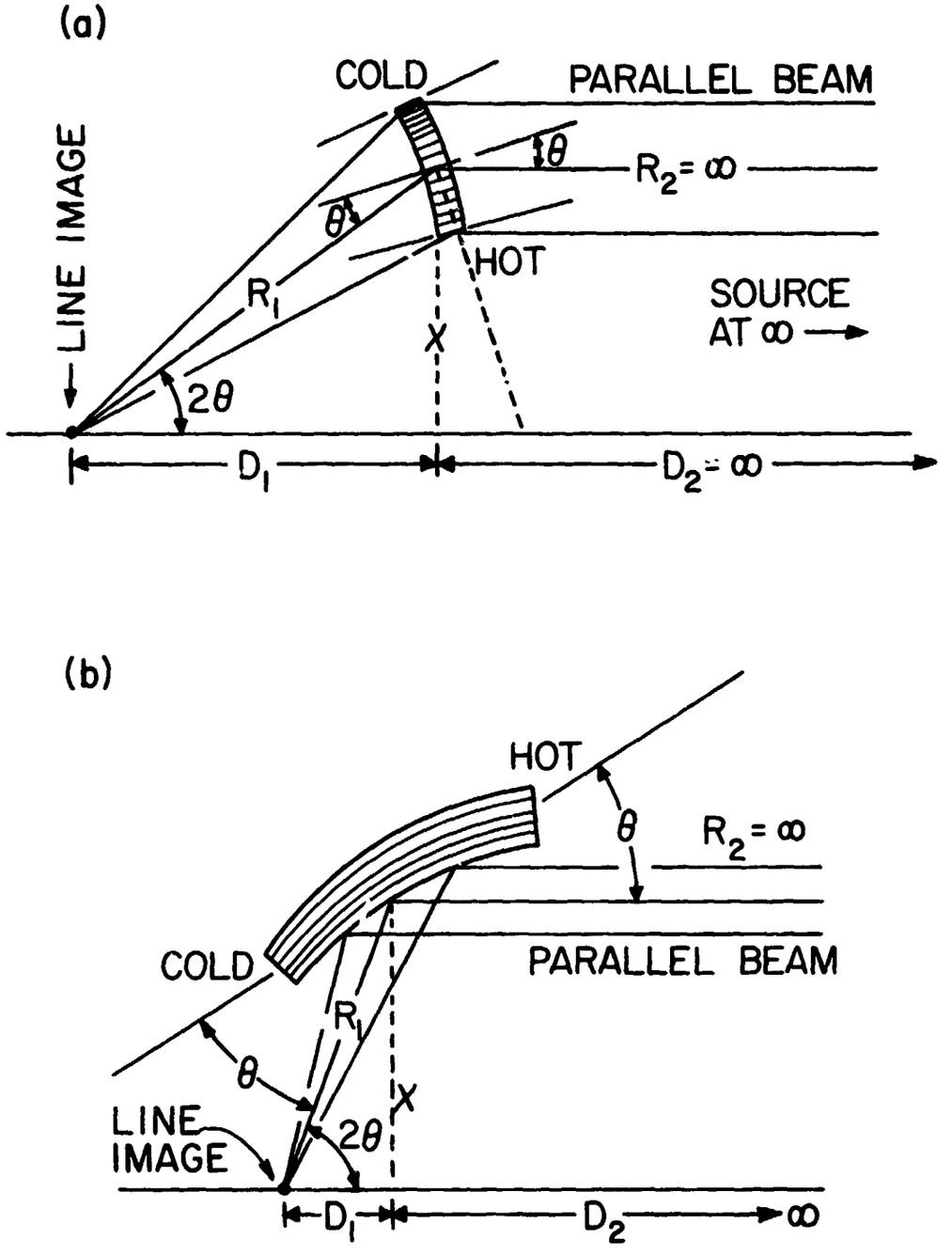


Fig. 5. Special case for parallel beams (source at inifinity) for the (a) transmission case and (b) reflection case of the new focusing method using bent crystals and thermal gradients. θ, x, $D_1$, $D_2$, $R_1$, and $R_2$ are the same as in Fig. 4

If a point focus is required as it might in an imaging telescope then a second crystal-diffraction element will be required to focus the beam in the plane at right angles to the first focusing plane. This requires that the second crystal element be rotated by 90° around the axis of the beam as is shown in Figure 6.

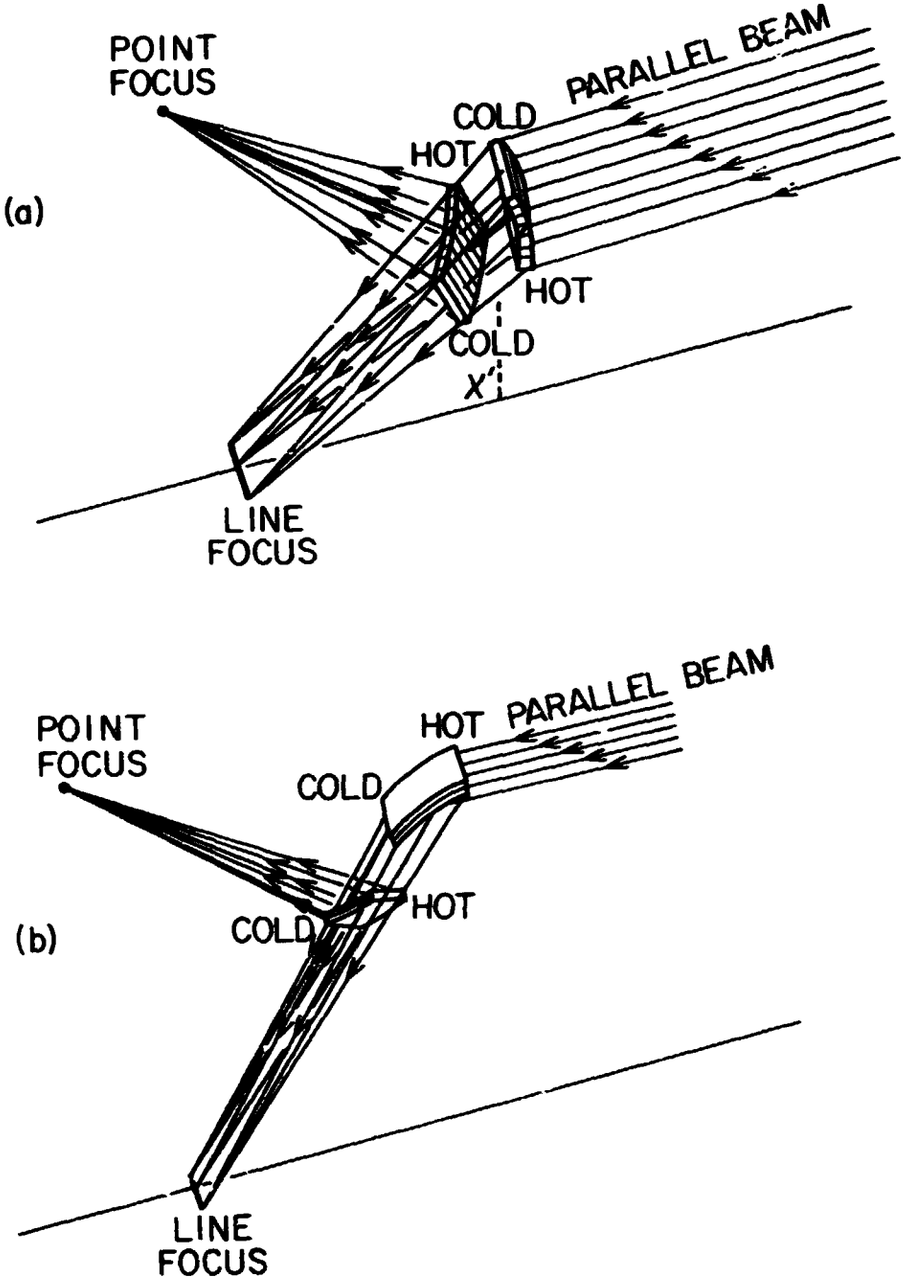


Fig. 6. Special case of double focusing of parallel beams for the (a) transmission case and (b) reflection case using the new bent crysta/thermal gradient method

A more elegant but more complicated method can be found to obtain double focusing with the reflection type diffraction crystal (Berreman, 1955).

This approach is shown in Figure 7 where the diffraction crystal is also bent in a second direction, in the plane perpendicular to the diffraction plane. Either type of double focusing opens up the possibility of doing good imaging with a space telescope that uses some sort of position sensitive focal plain detector.

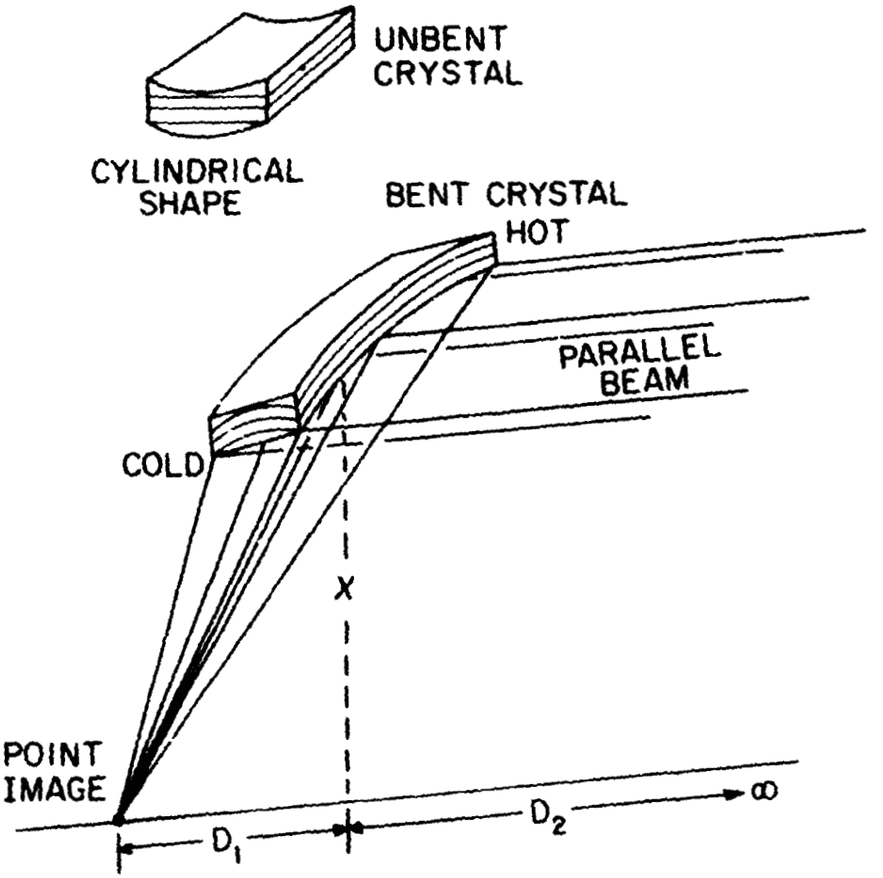


Fig. 7. Double focusing with a single crystal element that has been specially ground and shaped before bending and the application of a thermal gradient

In the parallel beam focusing case $D_2$ and $R_2$ approach infinity. This simplifies the expressions for $R_c$, $\Delta t/\Delta \ell$ or $\Delta d/\Delta \ell$ where $\Delta \ell$ is the distance along the surface of the crystal in the diffraction plane. $R_c$ in the transmission case is given by Eq. (7)

$$R_c = \frac{2R_1}{\cos \theta} \tag{7}$$

and Eq. (8) in the reflection case

$$R_c = \frac{2R_1}{\sin \theta} \tag{8}$$

Also $\phi = \theta$ and the fractional change needed in the crystal spacing $\Delta d/d$ is given by Eq. (9) for the transmission case,

$$\frac{\Delta d}{d} = \frac{\cos^2 \theta}{2R_1 \sin \theta} \Delta \ell \tag{9}$$

and for the reflaction case, Eq. (10)

$$\frac{\Delta d}{d} = \frac{\cos \theta}{2R_1} \Delta \ell \tag{10}$$

The corresponding thermal gradient needed for the transmission is

$$\frac{\Delta t}{\Delta \ell} = \frac{\cos^2 \theta}{2\alpha R_1 \sin \theta} = \frac{\cos \theta}{\alpha x} \cdot \frac{\sin 2\theta}{2 \sin \theta} \tag{11}$$

and in the reflection case

$$\frac{\Delta t}{\Delta \ell} = \frac{\cos \theta}{2\alpha R_1} = \frac{\cos \theta}{\alpha x} \cdot \frac{\sin^2 \theta}{2} \tag{12}$$

For small values of $\theta$ the thermal gradient approaches a constant $(1/\alpha x)$ for the transmission case. In the reflection case the thermal gradient goes to zero as $\theta$ approaches zero or 90°. Note that the "d" spacing of the crystal does not enter into these equations so they are quite general. Also, the minimum value $R_1$ or x that can be used is set by the maximum value allowable for $\Delta t/\Delta \ell$ where $\Delta \ell$ is the length along the crystal surface in the diffraction plane. Thus the minimum size of the spectrometer is set by the maximum permissible value of the thermal gradient, $\Delta t/\Delta \ell$. For $\theta = 20°$ and $\alpha = 1.34 \times 10^{-5}$ (Quartz) and $\Delta t/\Delta \ell = 200°C/cm$, $x_{min} = 329.5$ cm in the transmission case and $x_{min} = 112.7$ cm in the reflection case. For a $\Delta t/\Delta \ell$ of 100°C/cm they will be twice as big, etc. This means that a spectrometer that relys on a thermal gradient to change the "d" spacing will be large, especially for small values of $\theta$.

## III. DIFFERENT METHODS FOR CHANGING THE CRYSTAL PLANE SPACING

The above discussion has used a thermal gradient to vary the "d" spacing in the diffraction crystals. The range of Bragg angles over which the crystal will focus monochromatic radiation is limited by how large a temperature difference can be applied to the crystal. In principle one could apply a $\Delta t$ of 1000°C to a quartz crystal which would correspond to a $\Delta d/d = 1.34 \times 10^{-2}$ or 1.34%. In practice a $\Delta t$ of 300°C (-100°C to +200°C) is all one would like to consider. This would give a $\Delta d/d = 4 \times 10^{-3}$ or 0.4%. As discussed in the previos section, the minimum value of x, the distance of the crystal from the axis or baseline is determined by t' maximum value attainable for $\Delta t/\Delta \ell$ [see Eq. (11) and (12)] and sets a minimum size for the spectrometer. An alternate method for changing the "d" spacing is to grow a crystal composed of two types of atomic like Si and B or Si and Ge (Pearson, 1967), (Pearson, 1972), and (Smither, 1982) and change the relative fraction of each type of atom as a function of position in the crystal. The lattice spacing in a Si-Ge mixed-element crystal can be changed from a value of d = 5.434 for pure Si to a value of d = 5.657 for pure Ge. This change in "d" of 4.1% corresponds to a $\Delta t = 10^4$°C for the thermal gradient method for varying "d". This approach has the advantage of giving large values of $\Delta d/d$ and $\Delta\theta$ and at the same time not requiring the power needed to maintain the thermal gradients needed in the examples cited, previously. The main disadvantage of this approach is that it does not have the ability to change the spacing gradient during the experiment and adjust for the focusing of different wave lengths or the ability to scan over a line in the spectrum by just changing the average temperature of the diffraction crystal. If the two approaches are combined, both the large $\Delta\theta$ and the variable $\Delta d/\Delta \ell$ can be retained. The use of at least some thermal gradient is also important because it retains the ability to control and change the increment of wavelength, $\Delta\lambda$, that is focused at one position on the focal plane. The narrowest value of $\Delta\lambda$ is obtained when the $\Delta d/\Delta \ell$ is matched to the changing Bragg angle needed for a perfect focus. If the system is detuned by using an incorrect value for the $\Delta d/\Delta \ell$ then a range of wavelengths will be focused at the image spot. This will allow a search mode to be used in the instrument if the energy of the line is not well known. After the line is located then the value of $\Delta\lambda$ can be adjusted to give the best sensitivity and/or resolution.

## IV. APPLICATION TO A X-RAY TELESCOPE

A number of the special features of the new method, focusing monochromatic radiation, imaging, control of $\Delta\lambda$, line scanning, etc., could be quite useful in the design of an x-ray telescope. Although the method could be applied to the low energy x-ray region ($E_\gamma < 5$ keV) the considerable success of the grazing incident telescope like the one flown on the Einstein Observatory in this energy region make it more interesting to look at a telescope designed to look at radiation in the 10 keV to 200 keV range and the possibility of extending it to the 200-600 keV range. The fluxes at these higher energies are quite low so the collection area must be large, the order of square meters. This means that a large number of crystal elements will be needed that all contribute to the same focal spot. Figure 7 is a schematic

drawing of a large area telescope where the individual diffraction crystals are located on a large ring structure. Assuming crystals of 6 cm length (Radial direction) and 0.5 cm wide mounted on a ring 20 m in diameter and assuming a 20% loss in area for the support structure then this one ring will have an entrance aperature for the telescope of $3.0 \times 10^4 \times \cos \theta$ ($cm^2$) for the transmission case and $3.0 \times 10^4 \times \sin \theta$ ($cm^2$) for the reflection case. For small values of $\theta$ the transmission case or large values of $\theta$ in the reflection case the entrance aperature would be about 2.5 to 2.2 $m^2$ and never need be lower than 2.1 $m^2$. If 5 such crystal rings are used then the entrance

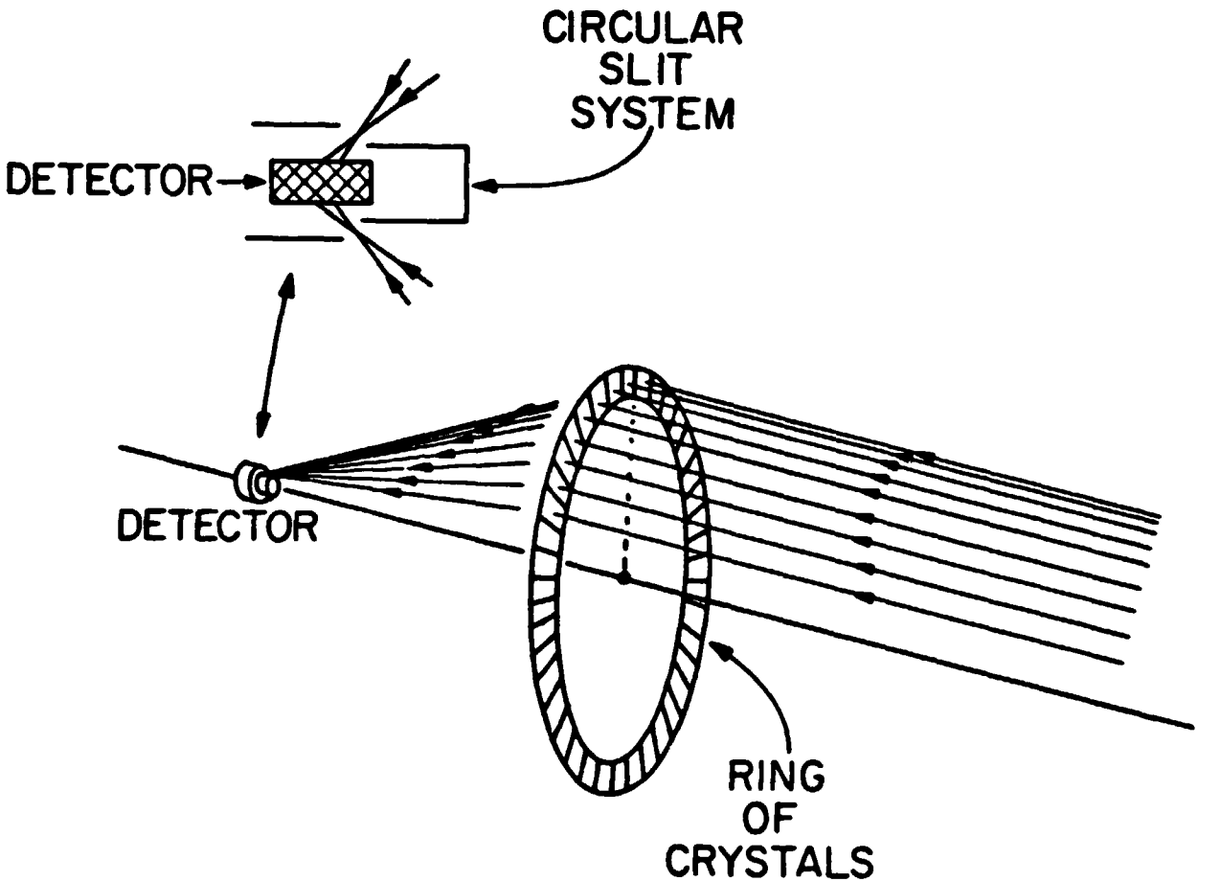


Fig. 8. Schematic drawing of a space telescope with a ring of diffraction crystals focusing a parallel beam into a circular slit. Details of the circular slit and detector are shown in the upper left

aperature will increase to 10.5 to 15 square meters or $\sim 10^5$ $cm^2$. If one uses high quality crystals then the through put of this system can be quite large due to the high reflectivity of the diffraction process. If one uses transmission crystals it is possible to select a thickness for the crystals that

maximizes the product of reflection of the crystal times the transmission through the crystal so that 30 to 40% of the incident monochromatic radiation is focused on the focal spot for any selected x-ray energy from 20 keV to 200 keV. At 500 keV the through put drops to 13%. Table I gives reflectivity and transmission coefficients for optimum thickness Quartz crystal based on measurements made on high quality quartz crystals at ANL. In principle, this

Table 1. Reflectivity and transmission coefficients for higher quality quartz crystal plates when used as transmission type diffraction crystals. The thickness of each plate has been optimized at each photon energy ($E_\gamma$) for the highest product of the reflectivity x transmission (Ref. x Trans.).

| $E_\gamma$ | Thickness (Opt.) | Reflectivity | Transmission | Ref. x Trans. |
|---|---|---|---|---|
| (keV) | (mm) | (%) | ($I/I_o$) | (%) |
| 10. | 0.04 | 45.5[a] | .825[a] | 37.6 |
| 20. | 0.22 | 48.2 | .872 | 42.0 |
| 50. | 1.45 | 48.5 | .897 | 43.5 |
| 100. | 4.50 | 46.6 | .829 | 38.6 |
| 250. | 20.0 | 42.7 | .670 | 28.6 |
| 500 | 30.0 | 25.7 | .499 | 12.8 |
| 1000. | 50.0 | 13.0 | .430 | 5.6 |

[a]Values extrapolated from data at higher energies.

approach could be extended down to 5 keV but the optimum thickness at these low energies becomes so thin that the crystals become difficult to handle and the use of reflection type crystals is more practical. A similar set of values can be obtained for the reflection case.Thus the effective collection area of the telescope for monochromatic radiation can be made the order of one third of the entrance aperature at any x-ray energy below 200 keV by choosing the right crystals and crystal thickness for the transmission case or by using the right crystals in the reflection case for x-rays with energies below 20 keV. This gives an effective collection area of 1.0 $m^2$ to 0.7 $m^2$ ($10^4$ to 7 x $10^3$ $cm^2$) for one ring and 5 $m^2$ to 3.5 $m^2$ for the 5-ring assemble. These are large effective areas and assume single crystal diffraction elements. If the crystals are bent in only one direction as in Figure 5, then a line focus will be obtained and the focused radiation from a large ring (Figure 8) would be spread over an image spot whose diameter is equal to the width of the individual diffraction crystals. A 0.5 cm width gives an area of the image spot = 0.2 $cm^2$. For a focal distance ($D_1$) of 10 m this corresponds to a spot whose angular diameter is 100 arc sec.

Better angular resolution (~10 arc sec) and energy resolution can be obtained by focusing the crystals on a circular slit as shown in the upper left of Figure 8. This approach has the disadvantage in that it will not allow imaging of extended sources. If better imaging is desired than was obtainable with the cylindrically bent crystals discussed above then a doubly bent crystal element (see Figure 7) will have to be used or two singly-bent crystals (see Figure 6). If the later is used the maximum through put will be reduced from (30% to 40%) to (10% to 16%). The much better focus however will greatly increase the photons/cm$^2$ and the signal to background ratio. The spot size will now depend on the quality of the diffraction crystals used and could have a diameter of a few arc sec which corresponds to an image diameter of 0.2 mm for a focal length of 10 m and an angular width of 4 arc sec. The price that must be paid for this high resolution is that the instrument will be highly monochromatic and only a very narrow band of wavelengths will be diffracted at one time. The value of $E_\gamma/\Delta E_\gamma = 2 \times 10^4$ at 6 keV for a 4 sec width and a 2.57 Å "d" spacing (quartz, 110). This corresponds to a diffraction width of 0.3 ev. At 60 keV, the above example gives $E/\Delta E = 2 \times 10^3$ or a width of 30 ev. The doppler broadened line width (FWHM) of 6 keV line in a plasma with $T = 10^7$ K would be 2.2 ev and for a 60 keV line the broadened line width would be 22 ev. The 60 keV case is match in $\Delta E$ to the doppler broadening quite well and even if the plasma temperature was $10^8$ K with the increased doppler width $\Delta\theta_D = 70$ ev, the loss would be less than a factor of 2. The resolution, $\Delta E$, would also be the right order of magnitude to measure the temperature of the source by measuring the line width. The 6 keV line is not matched very well to the doppler broadening and it may help to detune the diffraction crystal by changing the thermal gradient so that the $\Delta\theta$ is 16 arc sec rather than 4 arc sec. This would give a $\Delta E$ for the diffraction process of 1.2 ev which would be a better match to the doppler broadened line. The total peak counting rate would however remain the same because the gain in reflectivity at one energy is balanced by the loss at another. The important feature of this type of $\Delta E$ control is that there is no loss in resolution either in the diffraction phase or in the plane perpendicular to the diffraction plane. If $\Delta E$ is increased by using a crystal with a large mosaic structure the loss occurs in both planes. If the mosaic structure of the diffraction crystal is increased from 4 sec to 16 sec then the reflectivity of the crystal for a single wavelength is decreased by a factor of 4 as it was before but there is also an increase in the image spot size in the direction perpendicular to the diffraction plane. This second expansion in the plane perpendicular to the diffraction plane is often neglected in efficiency calculation but it can seriously reduce the signal to background ratio in a focal plane detector. The expansion of the image in this sideways direction is given by Eq. (13)

$$\Delta\theta_\perp = \Delta\theta_M \tan 2\theta \qquad (13)$$

where $\Delta\theta_M$ is the width of the mosaic structure. For values of $\theta = 22°$ ($E_\gamma = 6.4$ keV in the above example) it becomes equal to the mosaic structure width. In the above example this effect would expand the image size further and decrease the photons per cm$^2$ in the image spot by an additional factor of 4. This additional spreading of the image will not only reduce the signal to backgrond ratio and thus the sensitivity of the instru-

ment but also seriously interfere with the resolution of two nearby images. This image broadening effect is discussed more throughly in the next section.

## IV. IMAGING

The great success of the grazing incident telescope flown on the Einstien Observatory in generating high-resolution, two-dimensional images of extended sources has made everyone aware of the importance of imaging in x-ray astronomy. It is, therefore, of interest to see if the high resolution, monochromatic, x-ray telescope discussed above can be used to image extended sources. In most cases a diffraction crystal can be described as a collection of small nearly-perfect crystallites whose rocking curves or diffraction widths are much narrower than the width of the mosaic structure. In high quality quartz the diffraction width of these small crystallites can be the order of 0.1 arc sec for 50 keV radiation. The mosaic structure width is thus a measure of the misalignment of these small crystallites and for very monochromatic radiation from a distant point source only a small fraction of these crystallites will be available for diffracting the incoming beam. The rest will be orientated at angles that do not satisfy the Bragg condition. If the diffraction width of the crystallites were the only thing contributing to size of the image on the focal plane and the crystal had an overall mosaic structure ($\Delta\theta_M$) of 10 arc sec., then an image would be formed within this 10 arc sec range with 0.1 arc sec resolution. Unfortunately the crystallite diffraction width is not the only contributor to the image spot size. As was mentioned in the previous section the overall mosaic structure of the crystal spreads out the image spot in the direction prependicular to the diffraction plane. The amount of spreading is given by Eq. (13), where $\Delta\theta = \Delta\theta_M \tan 2\theta$. Even for small values of $\theta$ this spreading will be noticeable, ($\theta = 5°$, $\Delta\theta = 10 \times \tan 10° = 1.8$ arc sec) and for $\theta = 20°$ ($\theta = 22.5°$, $\Delta\theta = 10 \times \tan 45° = 10$ arc sec) or larger, the spread will be equal to or larger than the mosaic structure of the whole crystal and make it more difficult to resolve images in this direction. This effect is shown in Figure 9. The above examples assumed very monochromatic radiation. Most astronomical line sources have a finite line width either due to the life time of the x-ray or due to doppler broadening. In this case different subsets of crystallites will reflect different wavelengths at slightly different Bragg angles. This results in a spreading of the image spot in the diffraction plane. If the line is very broad then the spreading in this direction will approach the mosaic structure width. The image spot size for a range of values for $\theta$ is shown in Figure 10. Off-axis sources will also be imaged on the focal plane but with some distortion. For a single element focusing crystal like the one shown in Figure 7. The field of view is quite wide in the direction perpendicular to the diffraction plane (plane containing the source, center of the crystal and center of an axis image). For monocromatic radiation imaging in the diffraction plane is limited to an angular width similar to the mosaic structure. Images of sources with broad spectral lines will be formed in this off-axis direction within the range of angles that correspond to the spectral line width. If the telescope consists of a large ring of focusing crystals then some part of the ring will always be available for off-axis diffraction so large angular areas (10 min x 10 min) can be imaged with decreasing sensitivity as one moves farther off-axis. The distortion of these images will not be too great even if large diameter circular rings are used. For the case of a 20 m diameter ring, $\theta = 10°$, and an off-axis distance

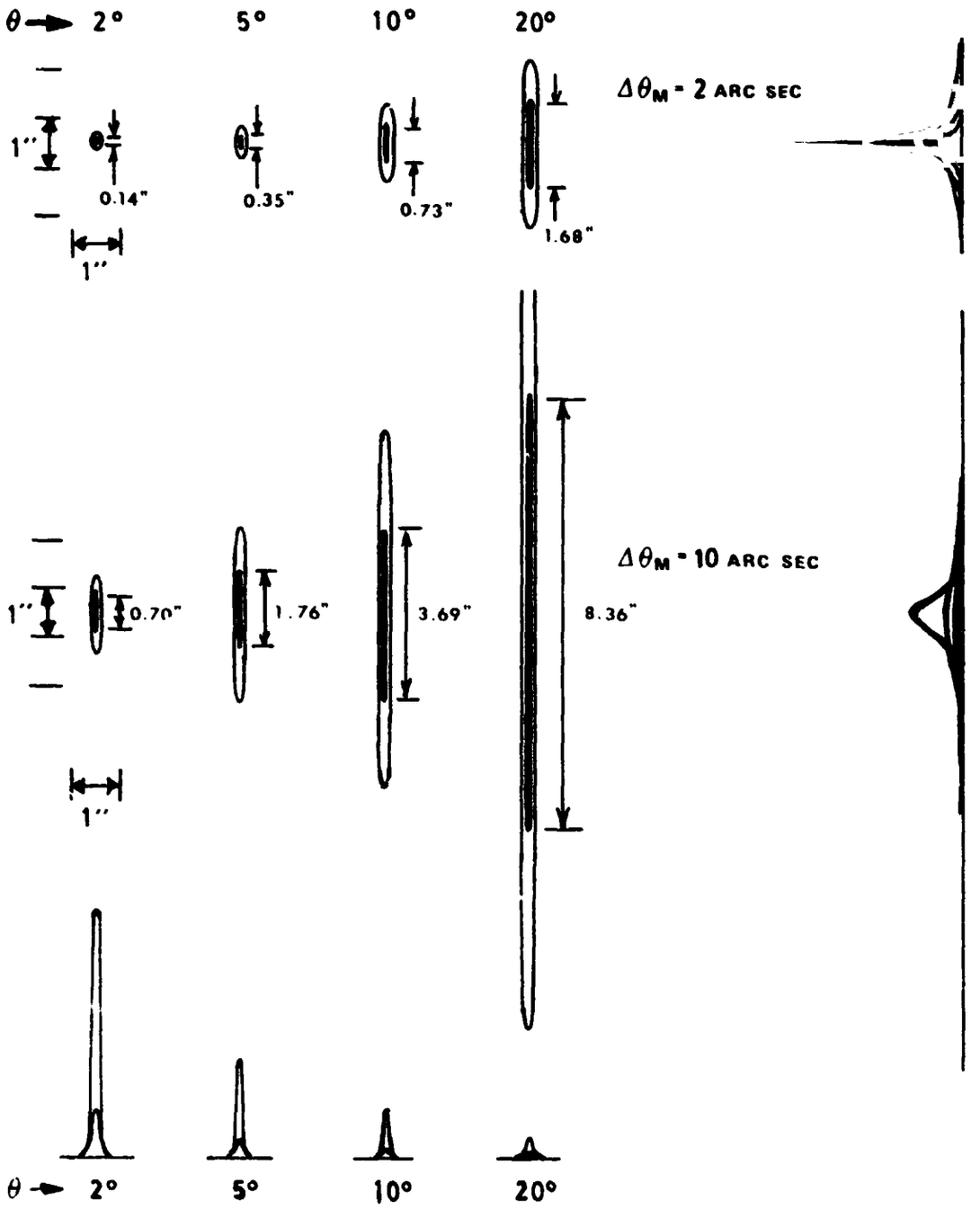


Fig. 9. Image spot size as a function of $\theta = 2°$, 5°, 10°, and 20° and mosaic structure width $\Delta\theta_M = 2$ sec and 10 sec for a double focusing single crystal system for a point source and monochromatic radiation. The solid filled area in the 50% height contour while the open line is the 10% height contour

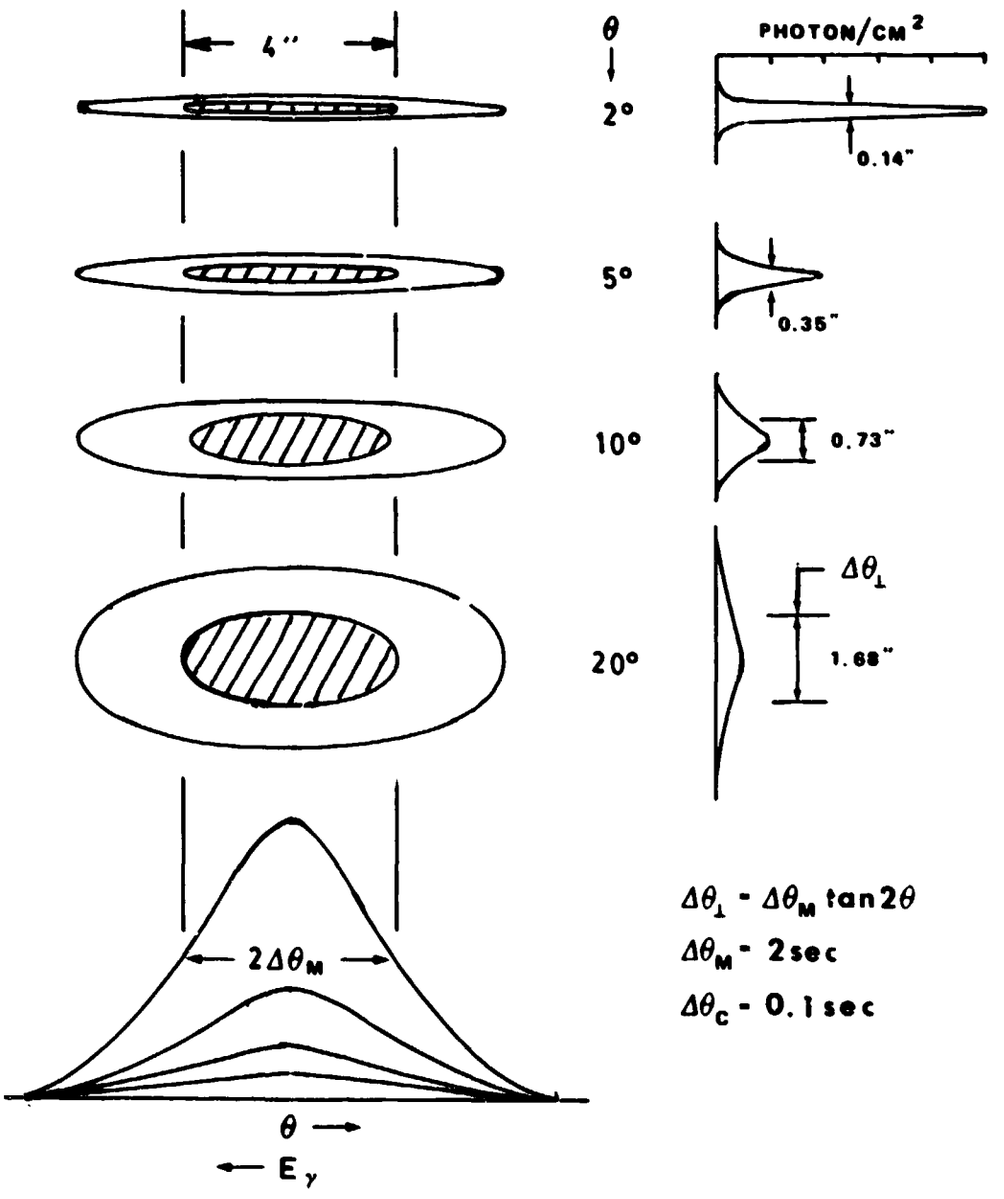


Fig. 10. Image spot size as a function of $\theta$ = 2°, 5°, 10°, and 20° for a single crystal system with a mosaic structure width $\Delta\theta_M$ = 2 sec when imaging continuum or very broad line sources from a distant point source. The shaded area is the 50% height contour while the outer ring is the 10% height contour.

of 20 arc sec the distortion of the image, $\Delta\psi_D$, is only 2.5 arc sec. In general $\Delta\psi_D$ given by Eq. (14)

$$\Delta\psi_D = \psi \sin 2\theta \tan 2\theta \qquad (14)$$

where $\psi$ is the off-axis angle of the source. Note that the angular distortion is not a function of the size of the instrument or the focal length and the ratio of $\Delta\psi_D/\psi_D$ is only a function of the Bragg angle $\theta$.

The use of a large circular ring of crystals generates an image spot that is a composite of the super imposed images from each crystal. This composite image can be generated from the single crystal images in Figures 9 and 10 by rotating these images through 360° aroung their centers. The off-axis images are generated in a similar way except that as the image rotates around its center, the center moves around a circle whose angular diameter ($\Delta\psi_D$) is given by Eq. (14). This distortion tends to disappear when the off-axis angle is large because the crystal elements responsible for the distortion are no longer at the right angle to diffract the beam. In many of the cases shown in Figures 9 and 10 the image is much larger in one dimension than the other and this rotation will generate an image with an appreciable larger area than the single crystal image. This will reduce the sensitive of the system and can considerably degrade the angular resolution. This image degradation can be partially eliminated by using narrow pie-shaped sectors covered with crystals rather than a continuous ring and focus each sector on a separate position sensitive detector. This would require the construction of sets of crystals with different average crystal spacings but it could improve the imaging at least in one direction by a factor of 5 to 10 depending on the angular width of the sectors (12° to 6°).

As mentioned above, if one increases $\Delta\theta_M$ in order to increase the range of wavelengths focused a spreading of the image in the direction perpendicular to the diffraction, $\Delta\theta_\perp$, also occurs. This loss in resolution and sensitivity can be avoided if one grows a reflection-type crystal so that the "d" spacing varies with depth into the crystal as well as with the position along the surface of the crystal. This variation of "d" with distance into the crystal has been used to increase the intregal reflectivity of a classical type instrument (see Figure 1) by varying the amount of Boron added to a silicon crystal grown epitaxially on a silicon crystal substrate (Fukuhara and Takano, 1980). The width of the diffraction peak was increased from a few arc sec for the undoped Si crystal to 80 sec for the epitaxial layer with graded Boron concentration that was 28 μm thick. This corresponds to fractional change $\Delta d/d = -10^{-3}$ and an enhancement of the rocking curve for the Cu $K_\alpha$ x-ray by a factor of 4 when using the 220 diffraction planes. The surface concentration of Boron was estimated to be $1.2 \times 10^{26}$ atoms/$m^3$ (0.24%).

## V. SUMMARY

The above discussion should not be considered as a formal proposal for an x-ray telescope but rather an illustration of the principals of the new focusing system and how it might be applied to the focusing and imaging of x-rays from a distant astronomical source. The real breakthrough for this application is the ability to image parallel beams (distant sources) of x-rays and the large con-

vergency angles that allow one to collect high energy x-rays from large areas without using impossibly long focal lengths.

The ability to change the width of the wavelength increment, $\Delta\lambda$, being diffracted without changing the image size and the ability to scan the line in wavelength without changing any of the physical dimensions of the instrument add to the attractiveness of this approach. The main design problems are how to apply thermal gradients to the bent crystals in a uniform and controllable manner and how to position and align a large array or ring of crystals to obtain the good resolution that is theoretically predicted.

## REFERENCES


1. Berreman, D. W., DuMond, J. W. M., and Marmier, P. E., 1954, R.S.I., 25, 1219.

2. Berreman, D. W., 1955, R.S.I., 26, 1048.

3. Canizares, C. R., Clark, G. W., Bardar, D., and Markert, 1977, SPIE, 106, 154.

4. Fukahara, A. and Takamo, Y., 1980, J. Appl. Cryst., 13, 391.

5. Johnson, H. H., 1931, Z. Phys., 69, 185.

6. Pearson, W. B., 1967, A Handbook of Lattice Spacings and Structure of Metals and Alloys, (Pergamon, New York, Vol. 1, 1958 and Vol. 2, 1967).

7. Pearson, W. B., The Crystal Chemistry and Physics of Metals and Alloys, (Wiley-Interscience, New York, 1972).

8. Smither, R. K., 1982, R.S.I., (to be published in the Feb. 1982 issue).